J. Cent. South Univ. (2012) 19: 1537−1542
DOI: 10.1007/s11771-012-1173-4

Springer

A novel grasping force control strategy for multi-fingered prosthetic hand

ZHANG Ting(张庭)[1], JIANG Li(姜力)[1], LIU Hong(刘宏)[1, 2]

1. State Key Laboratory of Robotics and System (Harbin Institute of Technology), Harbin 150001, China;
2. Institute of Robotics and Mechatronics, German Aerospace Center, Munich 82230, Germany

Abstract: A grasping force control strategy is proposed in order to complete various fine manipulations by using anthropomorphic prosthetic hand. The position-based impedance control and force-tracking impedance control are used in free and constraint spaces, respectively. The fuzzy observer is adopted in transition in order to switch control mode. Two control modes use one position-based impedance controller. In order to achieve grasping force track, reference force is added to the impedance controller in the constraint space. Trajectory tracking in free space and torque tracking in constrained space are realized, and reliability of mode switch and stability of system are achieved. An adaptive sliding mode friction compensation method is proposed. This method makes use of terminal sliding mode idea to design sliding mode function, which makes the tracking error converge to zero in finite time and avoids the problem of conventional sliding surface that tracking error cannot converge to zero. Based on the characteristic of the exponential form friction, the sliding mode control law including the estimation of friction parameter is obtained through terminal sliding mode idea, and the online parameter update laws are obtained based on Lyapunov stability theorem. The experiments on the HIT Prosthetic Hand IV are carried out to evaluate the grasping force control strategy, and the experiment results verify the effectiveness of this control strategy.

Key words: grasping; impedance control; force control; sliding mode control; prosthetic hand

1 Introduction

Bionic prosthetic hand often needs to apply the desired force in the operation of objects. Impedance control provides a unified framework for achieving compliant behavior when contacting with an unknown environment, which was extensively theorized by HOGAN [1]. The basic impedance control strategy is to regulate the relationship between force and position by setting suitable gains of impedance parameters. However, the basic impedance control fails to track desired force. So, the prosthetic hand fails to control grasping force by using basic impedance control strategy [2].

Impedance force control is one of the main force control algorithms in the literature with the hybrid position and force control [3−12]. Impedance function is realized by the relationship between force and position/ velocity error. After the pioneering work of the impedance control by HOGAN [1], there have been several major research issues to be solved on the impedance control. Within this impedance force control framework, many efforts have been made to solve these problems. Contact stability of the impedance control for stable execution of tasks has been analyzed [13]. In addition to these efforts, various control algorithms have been proposed. LASKY and HSIA [14] have proposed the inner/outer loop control scheme where the robot dynamics uncertainties are compensated by a robust position control algorithm in the inner loop and estimated environment position is modified using an integral control of force tracking error in outer loop. The generalized impedance control of considering a general dynamic relation between position error and force error to deal with the unknown environment stiffness has been proposed [15]. The adaptive techniques of using force tracking errors have been proposed to estimate environment stiffness or adjust controller gains to compensate for unknown environment stiffness [14]. LASKY and HSIA [14] have proposed a simple trajectory modification scheme using the robot controller to compensate for robot dynamics uncertainties as in Ref. [8] and environment stiffness is replaced by contact force information [15]. Later analysis has shown that accurate force tracking is not always guaranteed unless the accuracy of the estimated environment position is

Foundation item: Project(2009AA043803) supported by the National High Technology Research and Development Program of China; Project (SKLRS200901B) supported by Self-Planned Task of State Key Laboratory of Robotics and System (Harbin Institute of Technology), China; Project (NCET-09-0056) supported by Program for New Century Excellent Talents in Universities of China
Received date: 2011−04−06; **Accepted date:** 2011−10−19
Corresponding author: ZHANG Ting, PhD Candidate; Tel: +86−451−86412042; E-mail: zhangt.hit@gmail.com

within certain bounds [16]. Furthermore, JUNG et al [17] have proposed an intelligent force control algorithm using a neural network to compensate for uncertainties. Fuzzy-neuro techniques have been used for force control of unknown objects [18]. The adaptive technique has been used to minimize the force error directly [19].

The force-tracking impedance control algorithms can control force and do not switch drawback compared to force/position control algorithms. However, force-tracking impedance control algorithms fail to track desired position. It is important to control position and force precisely while grasping objects. So, a grasping force control strategy is proposed for multi-fingered prosthetic hand to improve a grasp performance, in which the environment has unknown dynamics. The position-based impedance control and force-tracking impedance control are used in free and constraint spaces, respectively. The fuzzy observer is adopted in transition in order to switch control mode. Two control modes use one position-based impedance controller. In order to achieve grasping force track, reference force is added to the impedance controller in the constraint space. In the control design, an adaptive sliding mode friction compensation method is used. This method makes use of terminal sliding mode idea to design sliding mode function.

2 Grasping force control strategy

The position-based impedance control and force-tracking impedance control are used in free and constraint spaces, respectively, as shown in Fig. 1. The fuzzy observer is adopted in transition in order to switch control mode. Two control modes use one position-based impedance controller. As shown in Fig. 1, M_t, B_t and K_t are diagonal symmetric positive definite matrices of desired inertia, damping and stiffness gains, respectively; θ_d, $\dot{\theta}_d$ are desired angle and desired angle velocity, respectively; K_P and K_D are position control gain and velocity control gain, respectively; u_{out} is impedance controller output; τ_r is adjusted torque; τ_d is desired torque; K_e is proportion gain; θ_r and $\dot{\theta}_r$ are direct current (DC) motor angle and DC motor angle velocity, respectively; θ_e is environment position.

The basic impedance control concept is to regulate the relationship between force and position by setting suitable gains of impedance parameters. The desired joint impedance mode of prosthetic hand fingers can be expressed as

$$\tau = M_t(\ddot{\theta}_d - \ddot{\theta}) + B_t(\dot{\theta}_d - \dot{\theta}) + K_t(\theta_d - \theta) \quad (1)$$

In the prosthetic hand system, the actual joint acceleration is received by the twice differential operations of the finger joint position sensor signal. The acceleration signal has great noise due to the position sensor noise, and may lead to the control system instability. Furthermore, the quality of prosthetic hand fingers is poor. So, M_t can be ignored, and Eq. (1) can be rewritten as

$$\tau = k_t(\theta_e - \theta) + b_t(\dot{\theta}_e - \theta) \quad (2)$$

The finger and environment constitute a new second-order impedance system, as shown in Fig. 2. In Fig. 2, k_e is desired environment stiffness gain.

The force-tracking error is given by

$$e_\tau = \tau_r - t_e = \tau_r - k_e(\theta_e - \theta) \quad (3)$$

Combining Eq. (3) with Eq.(2) yields the steady-state force-tracking error

$$e_{\tau ss} = \frac{k_t[\tau_r - k_e(\theta_e - \theta_r)] + k_e\tau_r}{k_t + k_e} \quad (4)$$

Define the equivalent stiffness as

$$k_{eq} = \left(\frac{1}{k_t} + \frac{1}{k_e}\right)^{-1} \quad (5)$$

Then, Eq. (4) can be rewritten as

$$e_{\tau ss} = k_{eq}\left[\frac{\tau_r}{k_e} - (\theta_e - \theta_r) + \frac{\tau_r}{k_t}\right] \quad (6)$$

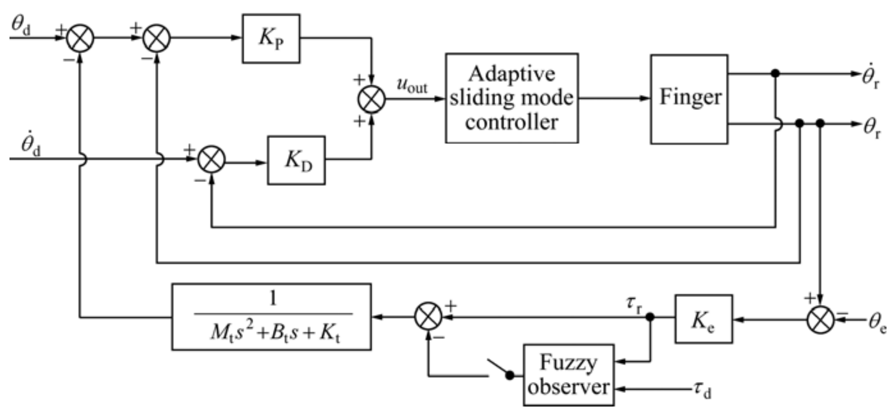

Fig. 1 Schematic of grasping force control strategy

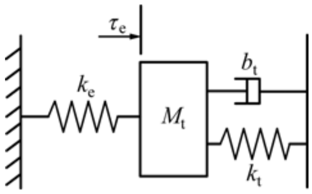

Fig. 2 Schematic diagram of contact impedance model for finger and environment

For the steady-state force-tracking error keeping zero, θ_r is satisfied as

$$\theta_r=\theta_e-\frac{\tau_r}{k_{eq}} \tag{7}$$

The environment stiffness k_e can be estimated by

$$\tau_e=k_e(\theta_e-\theta) \tag{8}$$

Combining Eq. (8) with Eq. (5) yields

$$k_{eq}=\frac{k_t\tau_e}{k_t(\theta_e-\theta)+\tau_e} \tag{9}$$

Combining Eq. (9) with Eq. (7) yields

$$\theta_r=\theta_e-\tau_r\frac{k_t(\theta_e-\theta)+\tau_e}{k_t\theta_e} \tag{10}$$

Define e=θ−θ_r, then the impedance control law input is given by

$$\tau_e=b_t\dot{e}+k_t e \tag{11}$$

Define ε=θ−θ_e, then e=ε+θ_e−θ_r. It has $\dot{\theta}_e=\dot{\theta}_r=0$ in constraint space. Then, Eq. (11) can be rewritten as

$$b_t\varepsilon+k_t(\varepsilon+\theta_e-\theta_r)=\tau_e \tag{12}$$

Consider $\tau_e\neq 0$ in constraint space, then Eq. (12) can be rewritten as

$$\theta_e-\theta_r=\tau_r\frac{k_t(\theta_e-\theta)+\tau_e}{k_t\tau_e} \tag{13}$$

Combining Eq. (13) with Eq. (12) yields

$$b_t\dot{\varepsilon}+k_t\varepsilon\left(1-\frac{\tau_r}{\tau_e}\right)=\tau_e-\tau_r \tag{14}$$

Considering τ_e=τ_r in constraint space, $b_t>2\sqrt{k_e}$ must be satisfied for tracking desired force.

In order to deal with environment changing, the new adaptive impedance equation is proposed as

$$b_t(\dot{\varepsilon}-w)=\tau_e-\tau_r \tag{15}$$

where $w(t)$ is online adjusted gain according to the grasping force control error. The proposed simple adaptive law is given by

$$w(t)=w(t-T_s)+\eta\frac{\tau_e(t-T_s)-\tau_r(t-T_s)}{b_t} \tag{16}$$

where T_s and η are sampling time and adaptive gain, respectively.

3 Position tracking control strategy

The mode of the prosthetic hand fingers joint can be expressed as

$$\begin{cases}\dfrac{\mathrm{d}\theta(t)}{\mathrm{d}t}=\omega(t)\\[2mm] \dfrac{\mathrm{d}\omega(t)}{\mathrm{d}t}=\dfrac{1}{T}\omega(t)+\dfrac{K\cdot K_\theta}{T}U-\dfrac{K\cdot K_\theta}{T}T_f\end{cases} \tag{17}$$

where θ is electric motor output angle; ω is DC motor angle velocity; U is control system input (the input voltage of DC motor); T is electrical time constant of motor; K is open-loop gain of finger system; T_f is nonlinear friction torque of finger system; K_θ is drive ratio.

The position error $e(t)$ is given by

$$e(t)=\theta_d(t)-\theta(t) \tag{18}$$

where $\theta_d(t)$ and $\theta(t)$ are desired position and actual position, respectively.

The non-linear friction model is given by

$$T_f(\dot{\theta})=T_c\,\mathrm{sgn}(\theta)+(T_s-T_c)\mathrm{e}^{(-\alpha|\dot{\theta}|)}\,\mathrm{sgn}(\dot{\theta}) \tag{19}$$

where α is a time constant; T_f is non-linear friction force; T_c and T_s are non-linear friction coefficients; sgn(·) is sign friction.

Define $a=\dfrac{1}{K\cdot K_\theta}$ and $b=\dfrac{T}{K\cdot K_\theta}$, then

$$\ddot{\theta}(t)=\frac{a\dot{\theta}(t)+U-T_f}{b} \tag{20}$$

Terminal sliding surface is given by

$$s(t)=ce^{q\cdot p}+\dot{e} \tag{21}$$

where c is a positive constant; p and q are positive odd numbers, satisfying $q<p$.

The period of control system that reaches to e=0 on the sliding surface is given by

$$t_s=\frac{p}{c(p-q)}|\mathrm{e}(\theta)|^{(p-q)/p} \tag{22}$$

where $e^{-a|\dot{\theta}|}$ satisfies $0<\mathrm{e}^{-a|\dot{\theta}|}\le 1$, and then

$$\left|(T_s-T_c)^{-a|\dot{\theta}|}\,\mathrm{sgn}(\dot{\theta})\right|\le T_{fm} \tag{23}$$

where T_{fm} is the maximum of interference.

The adaptive sliding mode control law is given by

$$U=-\hat{a}\dot{\theta}-\hat{b}u_c+\hat{T}_c\cdot\mathrm{sgn}(\dot{\theta})+\hat{T}_{fm}\cdot\mathrm{sgn}(s_\Delta(t)) \tag{24}$$

where $\hat{a}$, $\hat{b}$, $\hat{T}_c$ and $\hat{T}_{fm}$ are estimate parameters of a, b, T_c and T_{fm}, respectively; u_c is the auxiliary control input,

$s_\Delta(t)$ is the extension function of $s(t)$, and $s_\Delta(t)$ is given by

$$s_\Delta(t)=s(t)-\delta\cdot S_{\text{sat}}(\frac{s(t)}{\delta}) \tag{25}$$

where δ is the boundary layer coefficient; $S_{\text{sat}}(\cdot)$ is saturation function and given by

$$S_{\text{sat}}(x)=\begin{cases}x, |x|<1\\ \text{sgn}(x), |x|>1\end{cases} \tag{26}$$

Combining Eq. (25) with Eq. (26) yields

$$\begin{cases}\dot{s}_\Delta=s_\Delta=0, |s|<\delta\\ \dot{s}_\Delta=\dot{s}, |s_\Delta|=|s|-\delta, |s|>\delta\end{cases} \tag{27}$$

$$s_\Delta\cdot S_{\text{sat}}(\frac{s}{\delta})=|s_\Delta| \tag{28}$$

Combining Eq. (28) with Eq. (21) yields

$$\dot{s}=c\cdot\frac{q}{p}\cdot e^{\frac{q}{p}-1}\cdot\dot{e}-\frac{1}{b}[a\dot{\theta}-\hat{a}\dot{\theta}-\hat{b}u_{\text{c}}+\hat{T}_{\text{c}}\cdot\text{sgn}(\dot{\theta})+$$
$$\hat{T}_{\text{fm}}\cdot\text{sgn}(s_\Delta)-T_{\text{c}}\cdot\text{sgn}(\dot{\theta})-(T_{\text{s}}-T_{\text{c}})e^{-a\dot{\theta}}\cdot\text{sgn}(\dot{\theta})] \tag{29}$$

The auxiliary control input u_{c} is given by

$$u_{\text{c}}=-c\cdot\frac{q}{p}\cdot e^{\frac{q}{p}-1}\cdot\dot{e}-\ddot{r}-\beta\cdot s_\Delta \tag{30}$$

where β is positive constant.

The adaptive law is given by

$$\dot{\hat{a}}=-\eta_1\cdot\dot{\theta}\cdot s_\Delta \tag{31}$$

$$\dot{\hat{b}}=-\eta_2\cdot u_{\text{c}}\cdot s_\Delta \tag{32}$$

$$\dot{\hat{T}}_{\text{c}}=\eta_3\cdot s_\Delta\cdot\text{sgn}(\dot{\theta}) \tag{33}$$

$$\dot{\hat{T}}_{\text{fm}}=\eta_4\cdot|s_\Delta| \tag{34}$$

where η_1, η_2, η_3 and η_4 are adaptive law gains.

4 Experiment analyses

4.1 Experimental devices

The HIT Prosthetic Hand IV is composed of five active fingers, and each finger is actuated by one DC motor independently (15 DOF). The size of HIT Prosthetic Hand IV is nearly 158 mm × 76 mm, and 21 mm in thickness (palm), as shown in Fig. 3. The hand weight is nearly 440 g including actuators and circuits. The appearance of the fingers looks like that of a real human hand and the fingertips of index and thumb can exert 10 N grasping forces.

The hand is equipped with nine proprioceptive and exteroceptive analogue sensors: five position sensors (one for each finger), four force/torque sensors (measuring the grasping force of each finger except little finger), which is mounted at the base of finger, as shown in Fig. 4. All these signals are acquired by the local controller and will be available for feedback delivery to the patient through the user-prosthesis interface (UPI). Actuation units are also sensory equipped, since they are equipped with an integrated relative encoder (thrum, index and middle finger).

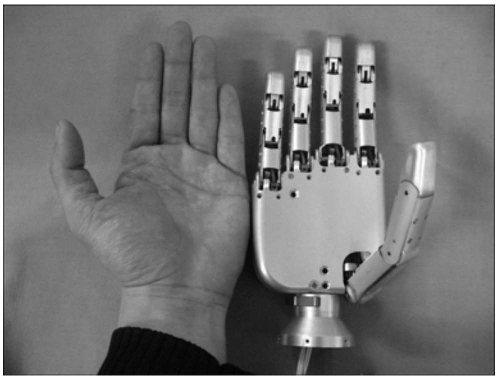

Fig. 3 HIT Prosthetic Hand IV

4.2 Experiment of adaptive sliding mode position control

To show the effectiveness of proposed grasping force method, the finger tracking the fold line trajectory was tested. The original angle is fixed at 58°. Figure 5 illustrates actual joint angles (dashdot lines) following desired joint trajectories (solid lines) of the finger and the position error, respectively. The results of experiment show the effectiveness of the proposed grasping force

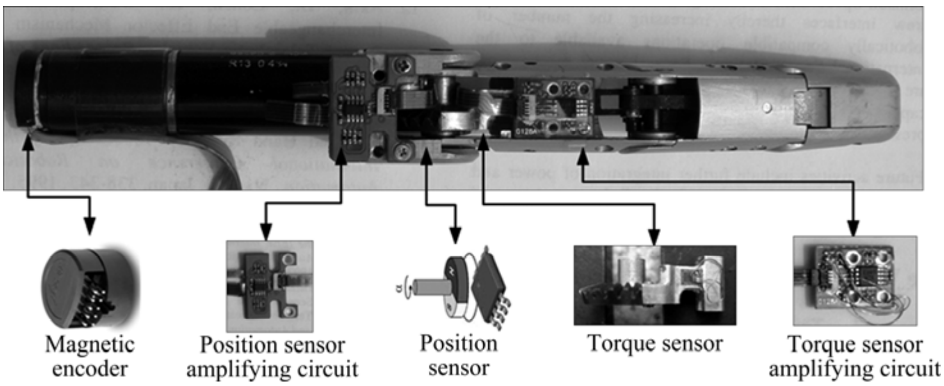

Fig. 4 Fingers of prosthetic hand

control method. The proposed grasping force controller exhibits much smaller position errors (see Fig. 5(b)), and therefore, exhibits better position control ability.

4.3 Experiment of grasping force control

To show the effectiveness of the proposed grasping force control method, the finger tracking the desired grasping force was further tested.

4.3.1 Step grasping force tracking experiment

Figure 6 illustrates actual grasping force (solid lines) following desired step grasping force (dashdot lines) of the finger and the position error, respectively. The results of experiment show the effectiveness of the proposed grasping force control method. The proposed grasping force controller exhibits much smaller force errors (see Fig. 6(b)), while a quite smooth grasping force track is obtained. It can be seen that small force appears overshoot just after contact and desired grasping force step change is reached.

4.3.2 Continuous grasping force tracking experiment

Figure 7 illustrates actual grasping force (solid lines) following desired continuous grasping force (dashdot

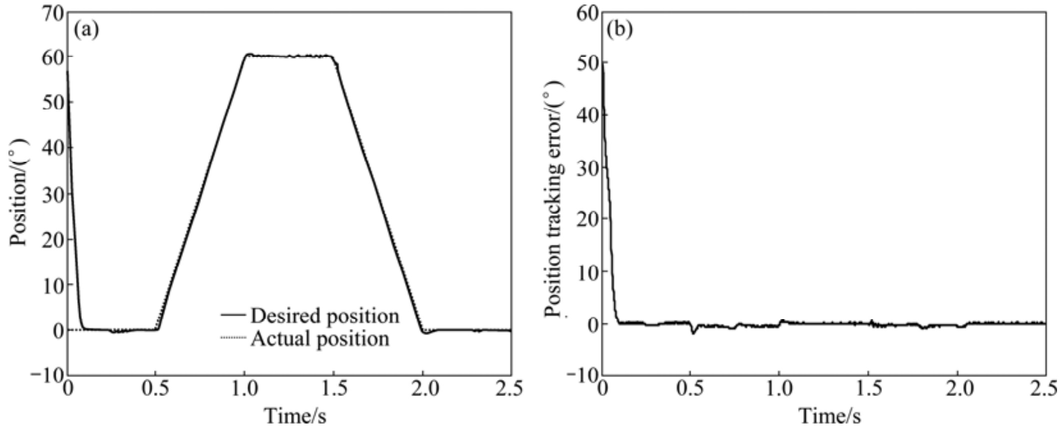

Fig. 5 Joint position control result: (a) Fold line trajectory tracking for free space motion; (b) Tracking errors in fold line trajectory tracking for free space motion

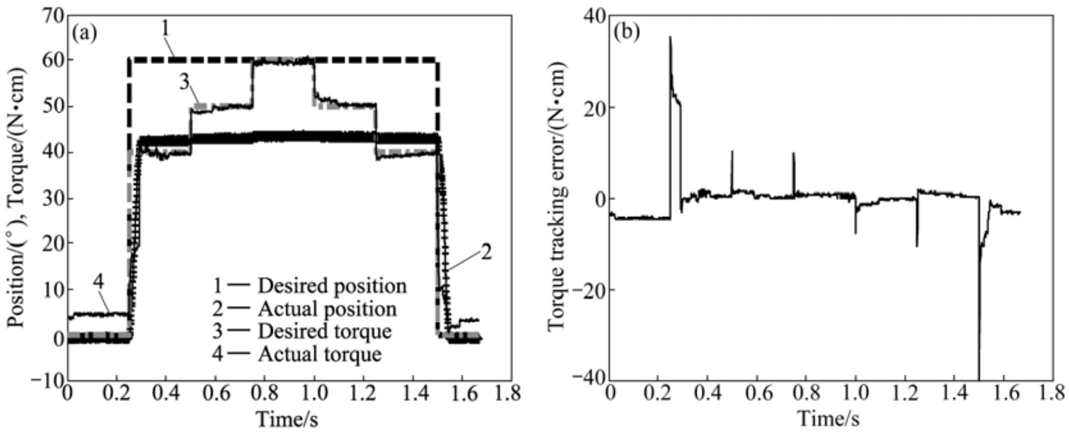

Fig. 6 Step grasping force tracking experiment: (a) Grasping force tracking; (b) Grasping force tracking errors

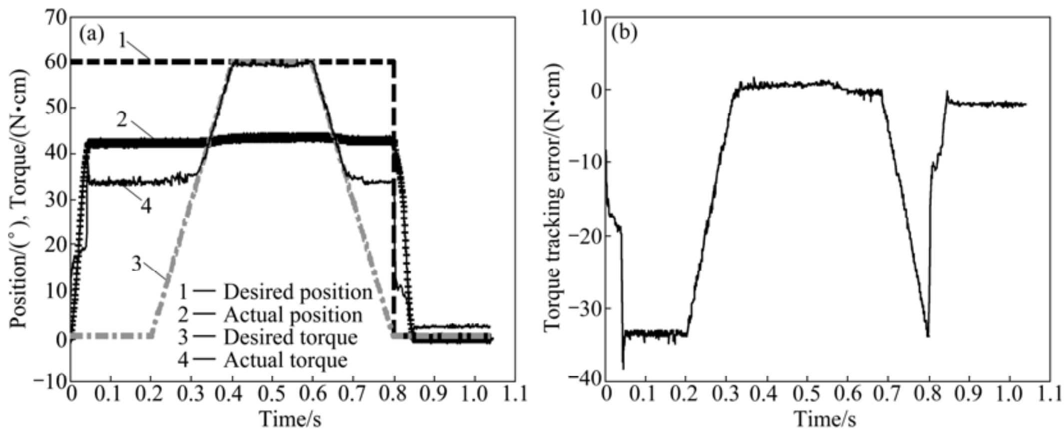

Fig. 7 Continuous grasping force tracking experiment: (a) Grasping force tracking; (b) Grasping force tracking errors

lines) of the finger and the position error, respectively. The results of the experiment show the effectiveness of the proposed grasping force control method. The proposed grasping force controller exhibits much smaller force errors (see Fig. 7(b)), while a quite smooth grasping force track is obtained. It can be seen that small force appears over-shoot just after contact is reached.

5 Conclusions

1) A grasping force control strategy is proposed in order to complete various fine manipulations by using anthropomorphic prosthetic hand. In the control design, the position-based impedance control and force-tracking impedance control are used in free and constraint spaces, respectively. The fuzzy observer is adopted in transition in order to switch control mode. The proposed grasping force control strategy is to stabilize position tracking and stabilize grasping force tracking, and small force over-shoot just after contact is reached.

2) It has been shown that the proposed adaptive sliding mode friction compensation method makes the position error converge to zero. This method uses terminal sliding mode idea to design sliding mode function, which avoids the problem of conventional sliding surface that position error does not asymptoticly converge to zero in finite time.

References

[1] HOGAN N. Impedance control: An approach to manipulator [J]. ASME J Dyna Syst, Measure, Control, 1985, 107(3): 1−24.

[2] ZHANG Ting, LI Kai, YANG Jing. Seam tracking control for mobile welding robot based on vision sensor [J]. Journal of Central South University of Technology, 2010, 17(6): 1320−1326.

[3] SERAJI H, COLBAUGH R. Force tracking in impedance control [C]// Proc IEEE Int Conf Robotics and Automation. Altanta: IEEE Process, 1993: 499−506.

[4] ERICKSON D, WEBER M, SHARF I. Contact stiffness and damping estimation for robotic systems [J]. The International Journal of Robotics Research, 2003, 22(3): 41−57.

[5] SERAJI H, COLBAUGH R. Force tracking in impedance control [J]. International Journal of Robotics Research, 1997, 16(1): 97−117.

[6] SINGH S, POPA D. An analysis of some fundamental problems in adaptive control of force and impedance behavior: Theory and experiments [J]. IEEE Transactions on Robotics and Automation, 1995, 11(6): 912−921.

[7] LOVE L, BOOK W. Environment estimation for enhanced impedance control [C]// Proceedings of the IEEE International Conference on Robotics and Automation. Belgium: IEEE Press, 1995: 1854−1859.

[8] JUNG S, HSIA T C, BONITZ R G. Force tracking impedance control of robot manipulators under unknown environment [J]. IEEE Transactions on Control Systems Technology, 2004, 12(3): 474−483.

[9] JUNG S, HSIA T C. Force tracking impedance control of robot manipulators for environment with damping [C]// The 33rd Annual Conference of the IEEE Industrial Electronics Society (IECON), Taipei, China, 2007: 2742−2747.

[10] JUNG S, HSIA T C. Neural network impedance force control of robot manipulator [J]. IEEE Transactions on Industrial Electronics, 1998, 45(3): 451−461.

[11] FARRELL T, WEIR R, HECKATHORNE C, CHILDRESS D. The effects of static friction and backlash on extended physiological proprioception control of a powered prosthesis [J]. J Rehabil Res Dev, 2005, 42(3): 327−342.

[12] LIGHT C, CHAPPELL P, HUDGINS B, ENGLEHART K. Intelligent multifunction myoelectric control of hand prostheses [J]. J Med Eng Technol, 2002, 26(4): 139−146.

[13] SANTIS D, SICILIANO B, LUCA A D, BICCHI A. An atlas of physical human–robot interaction [J]. Mechanism and Machine Theory, 2008, 43(3): 253−270.

[14] LASKY T, HSIA T C. On force-tracking impedance control of robot manipulators [C]// IEEE International Conference on Robotics and Automation. Sacramento: IEEE Press, 1991: 274−280.

[15] SCHERILLO P, SICILIANO B, ZOLLO L, CARROZZA M, GUGLIELMELLI M, DARIO P. Parallel force/position control of a novel biomechatronic hand prosthesis [C]// Proc 2003 IEEE/ASME Int Conf Adv Intell Mechatron. Como: IEEE Press, 2003: 920−925.

[16] DILLON G, HORCH K. Direct neural sensory feedback and control of a prosthetic arm [J]. IEEE Trans Neural Syst Rehabil Eng, 2005, 13(4): 468−472.

[17] JUNG S, YIM S B, HSIA T C. Experimental studies of neural networkimpedance force control for robot manipulators [C]// Proc IEEE Conf Robotics Automation. Seoul: IEEE Press, 2001: 3453−3458.

[18] KIGUCHI K, FUKUDA T. Position/force control of robot manipulatorsfor geometrically unknown objects using fuzzy neural networks [J]. IEEE Trans Ind Electron, 2000, 47(3): 641−649.

[19] SEUL JUNG, HSIA T C, BONITZ R G. Force tracking impedance control of robot manipulators under unknown environment [J]. IEEE Transactions on Control Systems Technology, 2004, 12(3): 474−483.

(Edited by DENG Lü-xiang)